Propagation of the overtide M_4 through the deep Atlantic Ocean

Richard D. Ray[1]

Received 7 August 2007; revised 13 September 2007; accepted 8 October 2007; published 6 November 2007.

[1] The nonlinear overtide M_4 is generated in shallow waters and is generally no more than a few mm amplitude in the deep ocean. Such small, periodic waves can now be mapped empirically by analyzing the long (15-year) time series of Topex/Poseidon and Jason-1 satellite altimetry. In a few locations of the deep Atlantic, M_4 amplitudes reach nearly 10 mm, confirming recent modeling efforts by Lyard and colleagues. These relatively large amplitudes evidently represent a complex interference pattern of free waves radiating from a few shallow sources, especially the Patagonian Shelf. They form approximately a standing-wave resonance in the Gulf of Guinea. **Citation:** Ray, R. D. (2007), Propagation of the overtide M_4 through the deep Atlantic Ocean, *Geophys. Res. Lett.*, *34*, L21602, doi:10.1029/2007GL031618.

1. Introduction

[2] The M_4 tide is a pure second harmonic (or overtide) of the principal lunar tide M_2. Its period is 6.2103 hours. It is formed in shallow water by nonlinear processes, attributable chiefly to nonlinearity in the continuity equation [*Le Provost*, 1991; *Walters and Werner*, 1991]. A linear component of M_4, caused by the fourth-degree term in the astronomical potential, is negligible in oceanic tides.

[3] M_4 is generally the largest of the quarter-diurnal tides. In some shelf locations it can attain large amplitude, e.g. over 30 cm [e.g., *Kwong et al.*, 1997]. In the deep oceans, however, it is generally observed to be no more than a few mm amplitude.

[4] *Lyard et al.* [2006] recently called attention to the fact that M_4 can reach amplitudes near 10 mm in several locations of the deep Atlantic Ocean, far from likely source regions. No comparable amplitudes were found in the Indian or Pacific Oceans. Their results are based on a purely numerical, time-stepping model (no observational constraints). Accurate simulation of M_4, especially its phases, can be exceedingly challenging. Independent confirmation of the Lyard et al. results would therefore be welcome.

[5] In fact, *Cartwright et al.* [1988] had previously pointed out anomalously large M_4 amplitudes in the Gulf of Guinea, based on bottom pressure and island gauge data. Their comprehensive survey of the whole Atlantic Ocean included an attempt to empirically map M_4 in the deep ocean. They established that the gross features of M_4 were completely independent of the parent M_2 tide, but the M_4 wavelengths were too short to allow them to produce an Atlantic cotidal chart.

[6] Satellite altimetry, especially the Topex/Poseidon mission, has played an essential role in determining our current knowledge of global tides. It has not previously been applied to mapping M_4 in the deep ocean, owing to the very small amplitudes. Yet as the time series of high-precision altimetry grows ever longer, it becomes feasible to examine such small tides. The purpose of this paper is to present the first empirical chart of M_4 in the deep ocean, based on satellite altimeter data. In keeping with Lyard et al., amplitudes in the Indian and Pacific Ocean are found to be very small, less than 4 mm (exceptions occur in the Mozambique Channel, the Arabian Sea, and west of the North Island of New Zealand). Therefore, this paper focuses on the Atlantic, where the anomalous amplitudes seen by Cartwright et al. and Lyard et al. are confirmed.

2. M_4 From Altimetry

[7] The work here continues a series of updated tidal analyses of Topex/Poseidon (T/P) and Jason-1 altimeter data, beginning with *Schrama and Ray* [1994] and continuing onwards with refined methodologies [e.g., *Ray*, 1999]. Inclusion of the M_4 constituent was thought warranted now because of (1) the lengthening T/P-Jason time series and (2) the availability of additional satellites to improve spatial resolution in shallow seas, including a 3-year T/P extension on a shifted ground-track. In the deep ocean, only T/P and Jason altimeter data are used here, but in shallow water data from ERS-1, ERS-2, and Geosat Follow-On are also added. A number of new improvements to the data have been incorporated: The T/P orbital ephemeris has been completely recalculated by *Luthcke et al.* [2003] with GRACE-based gravity models and the 2005 International Terrestrial Reference Frame. Data from ERS-1 and GFO have undergone adjustments [e.g., *Le Traon et al.*, 1995] to fold them more closely into agreement with T/P. New sea-state bias corrections and new relative altimeter biases have been computed for all satellites (B. Beckley, personal communication, 2007). To further reduce noise levels, non-tidal oceanographic signals have been removed from the data by employing the weekly multi-altimeter sea-surface elevation grids produced by the AVISO project at CNES/CLS [e.g., *Ducet et al.*, 2000]. (There are some minor instances of tidal contamination in these grids, mostly confined to wavelengths shorter than about 50 km. This could possibly reduce estimated M_4 amplitudes in shallow seas, but our deep-ocean solutions should be unaffected.)

[8] As given by *Schrama and Ray* [1994] the tidal analyses here are strictly empirical, with no hydrodynamic assimilation involved. But unlike Schrama-Ray, no prior hydrodynamic model is used to improve the short-wavelength fidelity of the recovered tide. This partly stems from the lack of a reliable global prior, but it was also done to discover how well M_4 can be determined completely from

[1]NASA Goddard Space Flight Center, Greenbelt, Maryland, USA.

This paper is not subject to U.S. copyright.
Published in 2007 by the American Geophysical Union.

empirical analyses. The altimeter data were subjected to quasi-independent tidal analysis in small geographical bins [e.g., *Cartwright and Ray*, 1990]. The bins are overlapping on a 0.5° grid (covering only the T/P latitude band ±66°), with deep-ocean bins fairly large (6° in longitude) but shortening considerably in shallower water, depending on the local bathymetry, the shape of the surrounding coastlines, and the number of nearby altimeter tracks. The 0.5° grid resolution is hardly adequate for mapping M_4 on continental shelves, and finer scale grids would be desirable in future solutions, assuming the coverage of available altimetry can support it. The resulting M_4 solution, shown as a cotidal chart in Figure 1, has been very heavily smoothed in the deep ocean, but much less so in shallows. In fact, in shallow water where the M_4 wavelengths are very short, almost any spatial smoothing tends to sacrifice accuracy, yet it is still necessary because to the inadequacy of sufficiently dense altimeter coverage.

[9] At any point along the T/P-Jason ground-track, M_4 can now be independently estimated with a standard error generally between 3 mm and 10 mm, depending on various factors such as background noise levels and data dropouts. In the deep ocean our binning methodology combines data from up to 4 independent tracks, plus an additional 4 or 5 tracks on the shifted T/P ground-track, thus reducing M_4 estimation error to below 5 mm, and more generally about 3 mm. Subsequent smoothing reduces this error further. Therefore, an assigned standard error of 1–2 mm for the deep-ocean regions of Figure 1 is not unreasonable. In shallow seas, owing to the smaller bin sizes, the relatively wide T/P track spacing, and the necessity of reduced smoothing, errors are at least an order of magnitude larger, often more.

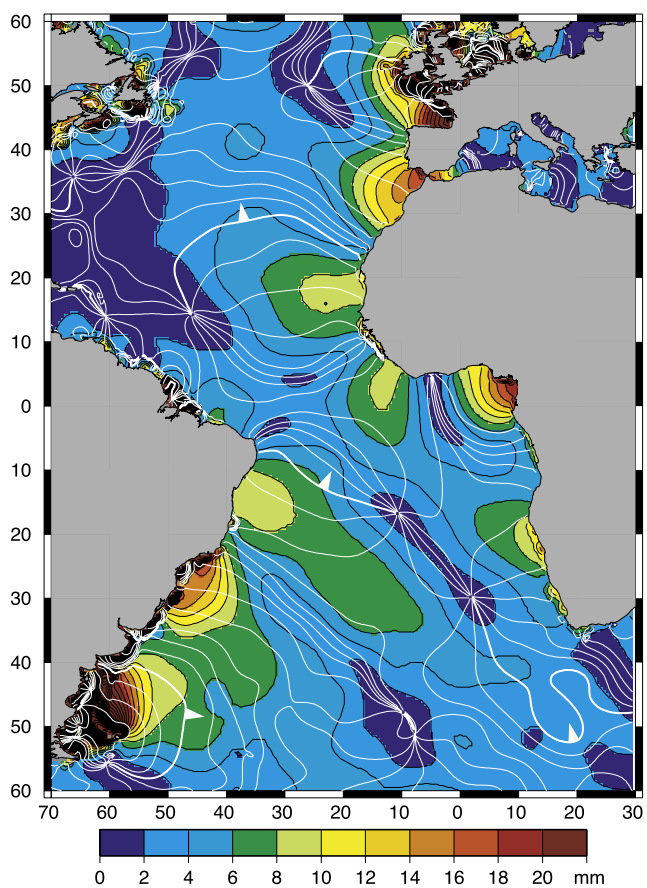

Figure 1. Cotidal chart of the M_4 tide in the Atlantic Ocean. Amplitude colors saturate in shelf regions. Phase contours given every 30°; the 0° isoline is slightly thicker and has a small arrow denoting sense of propagation.

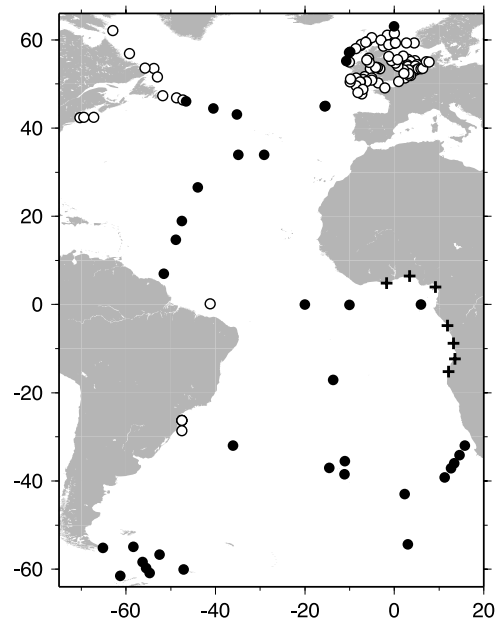

Figure 2. Locations of "ground truth" stations used for comparing M_4 tidal models. Circles correspond to stations used in Table 1. There are 92 shallow-water stations (open circles) and 40 deep-water stations (filled circles). All of the deep-water stations are based on bottom pressure measurements. Crosses correspond to seven coastal gauges used in Table 2.

[10] Comparisons against independent "ground truth" station data allow further assessment of the M_4 solution. A set of such stations, divided into deep and shallow-water stations, has been compiled and is shown in Figure 2. All of the deep-ocean stations are based on bottom-pressure records, most of them more than a year long. Many of these were extracted from the on-line datasets of the Global Undersea Pressure (GLOUP) archives, others are from the *Smithson* [1992] compilation, and nine others were determined here from original hourly data specifically for these M_4 tests. Bottom-pressure data also form many of the adopted shallow-water stations, but these have been supplemented with gauges on oil rigs (the North Sea) and small islands (e.g., Jersey in the English Channel). Table 1 summarizes the comparison statistics; a more complete tabulation is available as Data Set S1 of the auxiliary material.[1] These statistics are consistent with a deep-ocean standard error for the altimeter-derived M_4 of less than 2 mm. Note, however, that a single deep-ocean station with a very poor comparison is Cape Horn (55°S, 65°W), just south of the Patagonian Shelf, where our M_4 appears to be detrimentally affected by the smoothing between deep and

[1]Auxiliary materials are available at ftp://ftp.agu.org/apend/gl/2007gl031618.

Table 1. Statistics of M_4 Model and Ground-Station Differences[a]

Model	Deep-Water Stations RMS	Deep-Water Stations MAD[b]	Shallow-Water Stations RMS	Shallow-Water Stations MAD[b]
None	3.44	2.36	42.87	15.87
FES2004	2.78	1.65	46.76	14.92
This paper	1.66	0.61	25.51	5.77

[a]Differences measured in mm.
[b]MAD, median absolute difference.

shallow waters; without this site, the deep-ocean RMS would have been reduced to only 0.84 mm.

[11] The worst shallow-water comparisons occur at sites in the English Channel, where M_4 is very large (approaching 30 cm) and short wavelength. Our 0.5° grid resolution is completely inadequate for mapping in the Channel.

3. Discussion

[12] The Atlantic Ocean cotidal chart for M_4 (Figure 1) employs an amplitude color scale geared toward the deep ocean, so large amplitudes in shelf seas tend to saturate the scale. This includes the well-known high-amplitude regions on the European Shelf [e.g., *Kwong et al.*, 1997] and Patagonian Shelf [*Glorioso and Flather*, 1997]. Throughout most of the Atlantic many of the features found in the numerical model of *Lyard et al.* [2006] are here confirmed: a band of large-amplitude (~10 mm) tides spilling off the Patagonian Shelf into deeper waters, and, more intriguingly, a band of similarly large tides along the coast of west Africa, especially the Gulf of Guinea [see *Cartwright et al.*, 1988] and west of Gibraltar. The shallow-water source(s) of much of this M_4 energy is far from clear, although the phase contours clearly depict wave propagation northeastwards from Patagonia, extending across the equator, and continuing northwards into the latitudes of Europe.

[13] A noteworthy discrepancy with the Lyard et al. chart is the sense of propagation along the west coast of southern Africa. The Lyard et al. phases, like Figure 1 here, show propagation eastward along the coast of Ghana and Nigeria, but their wave then rounds the corner of the Gulf of Guinea and continues southwards along the coasts of Congo and Angola. In contrast, Figure 1 shows a northward propagating tide along the coasts of Angola and Congo, which, combining with the eastward-moving wave near Nigeria, forms a curious, almost standing-wave resonance in the Gulf of Guinea. At first glance, the Lyard et al. propagation might seem more realistic, since it mimics the propagation of M_2 (although with opposite sense of rotation around the Gulf). An analysis of tide-gauge stations along the African coast, however, agrees more closely with the altimeter results—see Table 2, wherein the tide-gauge phases are seen to decrease from Cameroon south to Angola. The fair correspondence between gauges and altimetry is rather remarkable given that the altimeter phases are being determined in spite of amplitudes well less than 1 cm at the four southernmost stations.

[14] To shed further light on the M_4 propagation across the Atlantic, Figure 3 presents a first approximation to a map of mean, barotropic energy fluxes. The required currents for such calculation are inferred from the elevations of Figure 1 by a least-squares inversion of the momentum and continuity equations [*Ray*, 2001]. Without reference to a detailed (high resolution) model of M_2, the forcing of M_4 in the momentum equations is unaccounted for, although it is surely confined to very shallow water. This modeling error does not appear to unduly influence deep-ocean currents so long as relatively large weights are applied to the continuity equation during inversion; open-ocean currents are then determined primarily by the locally measured elevation gradients and are fairly insensitive to distant boundary conditions or dissipation (or generation) assumptions [*Ray*, 2001]. The mean energy fluxes $\vec{F}$ follow from

$$F_i = \frac{1}{2}\rho g h u_i \zeta \cos\phi_i \tag{1}$$

Table 2. M4 Phase Lags, Clockwise Around the Gulf of Guinea[a]

Tide Gauge	Location		G_{gauge}	G_{alt}	G_{FES}
Takoradi, Ghana	4° 53′N	1° 45′W	314°	316°	324°
Lagos, Nigeria	6°25′N	3°25′E	344°	317°	356°
Douala, Cameroon	3°58′N	9°13′E	336°	324°	25°
Pte. Noire, Congo	4°48′S	11°51′E	296°	261°	51°
Luanda, Angola	8°47′S	13°14′E	190°	232°	83°
Lobito, Angola	12°20′S	13°33′E	166°	187°	104°
Mocamedes, Angola	15°12′S	12°08′E	165°	163°	120°

[a]All Greenwich phases lags G were estimated from multi-year time series of hourly tide-gauge data obtained from the University of Hawaii Sea Level Center, except for station Douala which is an older determination extracted from the International Hydrographic Bureau archives. Phases G_{FES} are from the numerical model of *Lyard et al.* [2006].

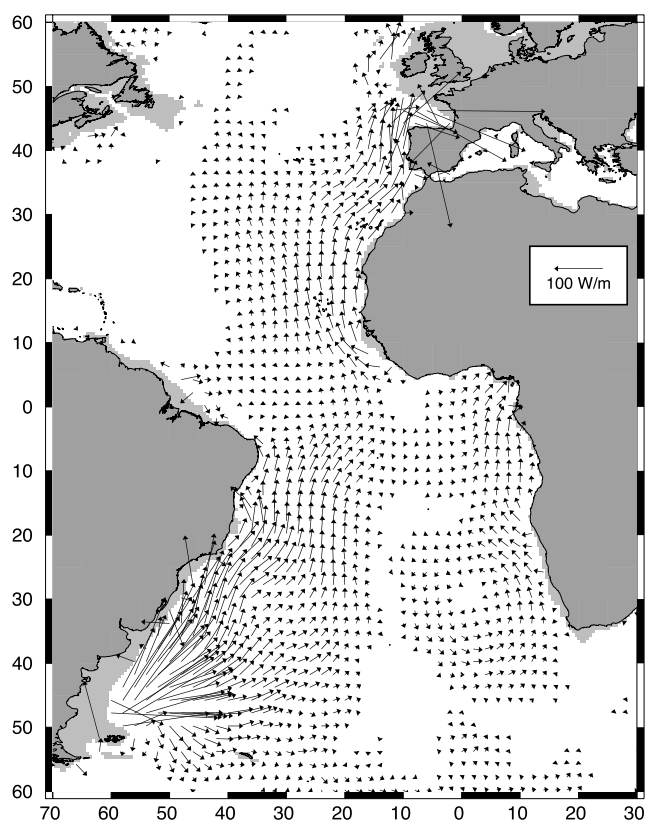

Figure 3. M_4 mean barotropic energy fluxes inferred from the data of Figure 1. Shallow-water fluxes are masked out; they are unreliable owing to insufficient spatial resolutions. For clarity, only every fourth vector in latitude and longitude is drawn. Vectors smaller than 6 W m^{-1} are not drawn.

$i = x, y$, where ρ is seawater density, g is acceleration of gravity, h is the water depth, ζ, $\vec{u}$ are the M_4 elevation and current velocity amplitudes, and ϕ is the phase difference between elevations and currents.

[15] One in situ confirmation of Figure 3 has been attempted. At 30°S, 42°W, a location of relatively large energy flux, two-year time series of current velocities from WOCE mooring array ACM3 is available [*Zenk et al.*, 1993]. A tidal analysis of one of these time series (water depth 3814 m; instrument depth 2614 m—hence, presumably mainly barotropic) gives u_x = (0.2 mm s^{-1}, 189°) eastward and u_y = (0.6 mm s^{-1}, 172°) northward velocity with standard error ± 0.1 mm s^{-1}. Combining with the elevations in Figure 1 yields an estimated energy flux $\vec{F}$ = (30, 120) ± 30 W m^{-1}. Figure 3 gives (28, 73) W m^{-1}, reasonably satisfactory agreement for fields of such high noise levels.

[16] Some aspects of Figure 3 are readily understood, others are more surprising. Figure 3 confirms very large flux of energy off the Patagonian Shelf, heading mostly eastwards in the south, and northeastwards in the north part of the shelf. An initial northeastward flux may well result from a Kelvin wave propagating away from the strong source region near 50°S [*Glorioso and Flather*, 1997], but this wave evidently combines with additional sources on the northern shelf to form a complex pattern of interfering waves.

[17] The near-standing wave pattern in the Gulf of Guinea is surprising but is apparently close to a quarter-wave resonance. The mean depth in the Gulf is 3400 m, so that $\sqrt{(gh)} \approx 180$ m s^{-1}, implying an M_4 quarter-wavelength of about 1000 km. The distance between the coast of Cameroon and the relatively tight cluster of M_4 phase lines surrounding the Gulf is not too far above 1000 km. In any event, the Gulf of Guinea clearly represents a sink, not a source, of M_4 tidal energy, with much of the energy evidently arriving from the south. The source of the latter is not clear; the African shelf in latitudes between 20°S and Capetown is not especially wide, and the M_4 amplitudes there (of order 10 mm) are not especially large for a shelf source. Yet there are no other obvious sources available. The intensification of M_4 energy fluxes in the mid-Atlantic near 10°N presents another mystery.

[18] An encouraging point, however, is that most (although not all) of these features are represented in the model of *Lyard et al.* [2006]. So further modeling investigations may well shed light on the pattern of waves evident in our Figure 1. Note too that Lyard's model is barotropic, which therefore eliminates baroclinic interactions as an important mechanism for these waves. In fact, the deep-water waves are surely free waves, radiating away from sources confined to a few very shallow seas. The situation is therefore considerably simpler than for linear tides with planetary-scale forcing. A study of the decay scales for these free, deep-ocean waves, and of the tradeoff between radiation and dissipation, would be of considerable interest.

[19] **Acknowledgments.** This work was supported by the NASA Ocean Surface Topography and GRACE projects. I thank Gary Egbert and Lana Erofeeva for discussions and for comparisons against their preliminary forward-model calculations. Tide gauge data were obtained from the University of Hawaii Sea Level Center, GLOUP data from the Permanent Service for Mean Sea Level, additional bottom-pressure data from Deirdre Byrne, and current velocity data from www.cmrecords.net.

References

Cartwright, D. E., and R. D. Ray (1990), Oceanic tides from Geosat altimetry, *J. Geophys. Res.*, *95*, 3069–3090.

Cartwright, D. E., R. Spencer, J. M. Vassie, and P. L. Woodworth (1988), The tides of the Atlantic Ocean, 60°N to 30°S, *Philos. Trans. R. Soc. London, Ser. A*, *324*, 513–563.

Ducet, N., P.-Y. Le Traon, and G. Reverdin (2000), Global high-resolution mapping of ocean circulation from Topex/Poseidon and ERS-1/2, *J. Geophys. Res.*, *105*, 19,477–19,498.

Kwong, S. C. M., A. M. Davies, and R. A. Flather (1997), A three-dimensional model of the principal tides on the European Shelf, *Prog. Oceanogr.*, *39*, 205–262.

Glorioso, P. D., and R. A. Flather (1997), The Patagonian Shelf tides, *Prog. Oceanogr.*, *40*, 263–283.

Le Provost, C. (1991), Generation of overtides and compound tides, in *Tidal Hydrodynamics*, edited by B. B. Parker, pp. 269–295, John Wiley, New York.

Le Traon, P.-Y., P. Gaspar, F. Bouyssel, and H. Makhmara (1995), Using Topex/Poseidon data to enhance ERS-1 data, *J. Atmos. Oceanic Technol.*, *12*, 161–170.

Luthcke, S. B., N. P. Zelensky, D. D. Rowlands, F. G. Lemoine, and T. A. Williams (2003), The 1-centimeter orbit: Jason-1 precise orbit determination using GPS, SLR, DORIS, and altimeter data, *Mar. Geod.*, *26*, 399–421.

Lyard, F., F. Lefèvre, T. Letellier, and O. Francis (2006), Modelling the global ocean tides: Modern insights from FES2004, *Ocean Dyn.*, *56*, 394–415.

Ray, R. D. (1999), A global ocean tide model from Topex/Poseidon altimetry: GOT99.2, *NASA Tech. Memo. 209478*, 58 pp., Goddard Space Flight Cent., Greenbelt, Md.

Ray, R. D. (2001), Inversion of oceanic tidal currents from measured elevations, *J. Mar. Syst.*, *28*, 1–18.

Schrama, E. J. O., and R. D. Ray (1994), A preliminary tidal analysis of Topex/Poseidon altimetry, *J. Geophys. Res.*, *99*, 24,799–24,808.

Smithson, M. J. (1992), Pelagic Tidal Constants 3, *IAPSO Publ. Sci. 35*, 191 pp., Int. Union of Goed. and Geophys., Boulder, Colo.

Walters, R. A., and F. E. Werner (1991), Nonlinear generation of overtides, compound tides, and residuals, in *Tidal Hydrodynamics*, edited by B. B. Parker, pp. 297–320, John Wiley, New York.

Zenk, W., T. J. Müller, and N. G. Hogg (1993), *Meteor* finishes her second DBE cruise, *WOCE Newsl. 14*, pp. 4–7, WOCE IPO, Deacon Lab., Wormley, U. K.

R. D. Ray, NASA Goddard Space Flight Center, Code 698, Greenbelt, MD 21114, USA. (richard.ray@nasa.gov)